ADVANCED MATERIALS

DOI: 10.1002/adma.200800497

Self-Assembly of Silver Nanoparticles Synthesized by using a Liquid-Crystalline Phospholipid Membrane**

By *Nuri Oh, Jung H. Kim,* and *Chong S. Yoon**

The increasing academic interest in nanotechnology is partially driven by the ever-growing demand for high-density data storage, high-speed computing, and high-performance displays. Owing to limits imposed by physical laws, these demands are increasingly difficult to fulfill using conventional semiconductor technology. Most of the developments in nanotechnology over the past decade have been dedicated to the synthesis of nano-objects.[1] Monodisperse nanoparticles have been produced through various chemical and physical routes including pyrolysis of organometallic compounds, solution chemistry, gas-phase reactions, metal–organic chemical vapor deposition, and electro-deposition.[2–7] Bio-inspired methods that use viruses and genetically engineered bacteriophages have been also employed to prepare nanometer-sized structures.[8] Key to the successful application of nanotechnology on an industrial scale, however, is the ability to manipulate these nano-objects into a spatially ordered pattern. Over the years, various physical, chemical, and biological methods for self-organizing nanoparticles have been proposed. Traditional lithographic patterning or guided assembly using an electron beam (or extreme ultraviolet interference lithography (EUV-IL) can consistently achieve a highly ordered two-dimensional superlattice of nanoparticles.[1,3,9] Because of the low throughput and high capital investment, various organic[3b,10] and biochemical molecules[11] including deoxyribonucleic acid have been used to drive the self-assembly of chemically produced monodisperse nanoparticles. These methods rely upon organic molecules such as alkylthiol to encapsulate the nanoparticles by chemi-adsorbing onto the particle surface. In addition to protecting the nanoparticles from irreversible aggregation, these capping molecules provide the necessary binding force for forming the superlattice through van der Waal interactions.[12] Alternatively, self-assembly of nanoparticles without the capping molecules has been recently developed. The method utilizes charge stabilized nanocrystal colloids to spontaneously self-assemble at the water/oil interface.[13]

In recent years, interest in using biomolecules, such as crystalline S-layer proteins and ferritin protein cages, as templates to scaffold inorganic nanostructures has arisen.[1] Of the various biomolecules, phospholipids, owing to the strong amphiphilicity stemming from possessing both polar heads and aliphatic tails, are able to spontaneously arrange themselves along a phase boundary or external surface.[14] This property permits the generation of a multitude of microscopic structures, that is, micelle, vesicle, bilayer, microtubules, and nanotubes, and would also render the phospholipid an ideal material to drive the assembly of metal nanoparticles.[15] Lipid nanotubes and solid-supported lipid multilayers were used to induce the self-assembly of the metal particles.[16]

In this Communication, we propose a novel method of using a solid-supported liquid crystalline lipid membrane as a template to synthesize nanometer-sized particles as well as to force the encapsulation of the resulting particles with lipid molecules. In the multilayer formed by lipids in the liquid-crystalline state, the lipid membrane becomes flexible as a result of chain melting.[14] Capitalizing on the flexibility of the liquid-crystalline lipid membrane, when metal film was deposited onto the liquid-crystalline lipid multilayer, the flexible lipid membrane allows penetration of the metal and subsequent formation of metal nuclei within the multilayer membrane. Subsequent spontaneous encapsulation of metal particles by the lipid molecules would limit the further growth of metal particles beyond an equilibrium size by confining the volume and shape of the metal particles. The unique aspect of our approach lies in the fact that the encapsulating lipid molecules are highly mobile and thus able to induce redistribution of metal to produce monodisperse nanoparticles. The mobility of the lipid molecules also expedites the formation of highly ordered nanoparticle superlattices. The diagram in Figure 1 illustrates the described process of forming a nanoparticle superlattice using the solid-supported liquid crystalline lipid membrane.

Figure 2a shows typical UV-vis spectra obtained immediately after deposition of Ag using a thermal evaporator onto the 1,2-dioleoyl-sn-glycero-3-phosphatidylcholine (DOPC) and 1,2-dipalmitoyl-sn-glycero-3-phosphatidylcholine (DPPC) multilayer prepared on fused silica substrates. The spectrum of the DOPC multilayer contains a broad extinction band centered at 432 nm with a full-width-at-half-maximum of 84 nm. The extinction band arose from the surface plasmon resonance of Ag nanoparticles, which is a characteristic feature of nanometer-sized Ag particles.[17] In fact, the resonance peak position closely matches one generated by an array of monodisperse Ag nanoparticles 4 nm in size.[12] The spectrum from the DPPC sample exhibited a nearly flat spectrum,

[*] Prof. C. S. Yoon, N. Oh, J. H. Kim
Division of Materials Science Engineering
Hanyang University
17 Haengdang-dong, Seongdong-ku, Seoul, 133-791 (Korea)
E-mail: csyoon@hanyang.ac.kr

[**] This work was supported by the Ministry of Science and Technology through the Nanoscopia Center of Excellence at Hanyang University. Supporting Information is available online from Wiley InterScience or from the authors.

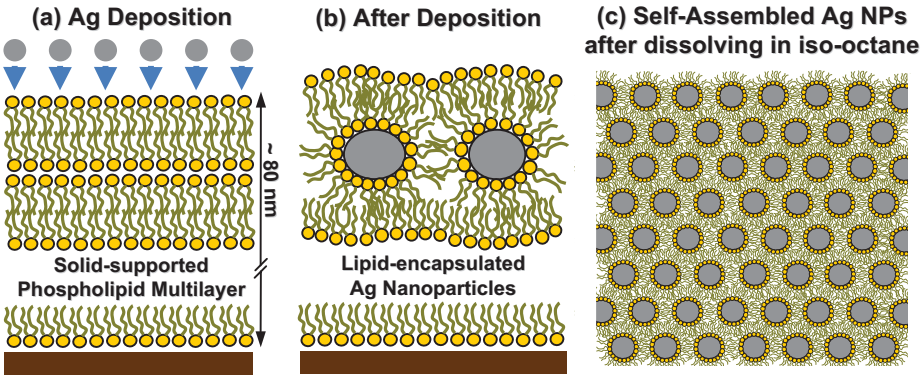

Figure 1. Diagram illustrating the formation process of the lipid-encapsulated Ag nanoparticle superlattice. a) Ag deposition onto the solid-supported lipid multilayer. b) Formation of lipid-encapsulated Ag nanoparticles. c) Superlattice of Ag nanoparticles produced by self-assembly of lipid molecules after dissolving the nanoparticle-embedded 1,2-dioleoyl-sn-glycero-3-phosphatidylcholine membrane in iso-octane.

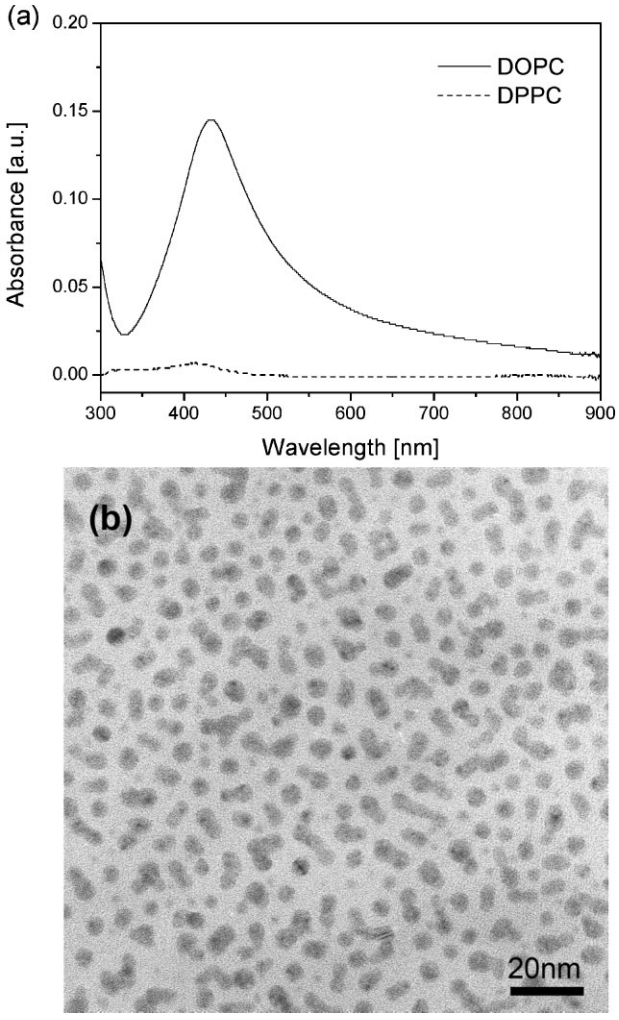

Figure 2. Optical properties and morphology of the Ag-embedded lipid membrane. a) UV-vis spectra after the deposition of Ag on the DOPC and DPPC multilayer. b) Transmission electron microscopy image of the as-deposited Ag nanoparticles embedded in the DOPC multilayer.

indicating that the substrate was transparent with a minimal amount of Ag deposited on the membrane. To confirm the presence of Ag nanoparticles in the as-deposited state, the DOPC multilayer was directly prepared on a transmission electron microscopy (TEM) Cu grid coated with an amorphous carbon thin film onto which Ag was deposited. A TEM image of the DOPC membrane after Ag deposition, shown in Figure 2b, confirms that Ag formed a monolayer of well-separated nanoparticles embedded within the DOPC multilayer, verified by cross-sectional TEM. Some of the particles appear elongated as a result of the agglomeration of several particles. On the other hand, in agreement with the optical spectrum, the DPPC membrane sample did not contain any Ag particles as the rigid membrane prevented nucleation of the metal particles within the multilayer. When the Ag film was deposited with increasing thickness above 50 nm, a nearly continuous thin film was eventually formed on the DPPC membrane. Similar results were obtained when prefabricated FePt particles were deposited onto both DOPC and DPPC multilayers. The FePt particles were unable to penetrate the rigid DPPC multilayer owing to the rigid lipid molecules, whereas the FePt particles were found embedded within the liquid-crystalline DOPC multilayer.[18]

Computer simulation showed that nanoparticles strongly interact with the lipid membrane and the lipid molecules spontaneously encapsulate the metal particle when introduced onto a lipid bilayer.[19] We believe that the Ag particles in Figure 2b are completely encapsulated by the DOPC molecules. In fact, X-ray photoelectron spectroscopy analysis of the DOPC sample (included in the Supporting Information) suggests that Ag atoms on the surface are covalently bound to the DOPC head group. Because the lipids are chemically bound to the Ag particle surface, it is conjectured that relatively high mobility of lipids will allow further manipulation of the Ag nanoparticles to tighten the particle size distribution and to possibly form 2D or 3D structures. Hence, the Ag-embedded DOPC membrane was heat treated at 80 °C in air for 3 h.

Figure 3 compares atomic force microscopy (AFM) images of the lipid membrane before and after heat-treatment. Prior to Ag deposition, the membrane was nearly flat with occasional voids and a surface step of which the height (4.1–4.2 nm) well-matched the length of a single lipid molecule. The total lipid multilayer thickness was ca. 80 nm, also confirmed by X-ray reflectivity measurement. The Ag deposition, however, drastically altered the surface morphology of the DOPC membrane, developing a cheese-like structure as can be seen from Figure 3b. The voids of ca. 1 μm were likely created from

ADVANCED MATERIALS

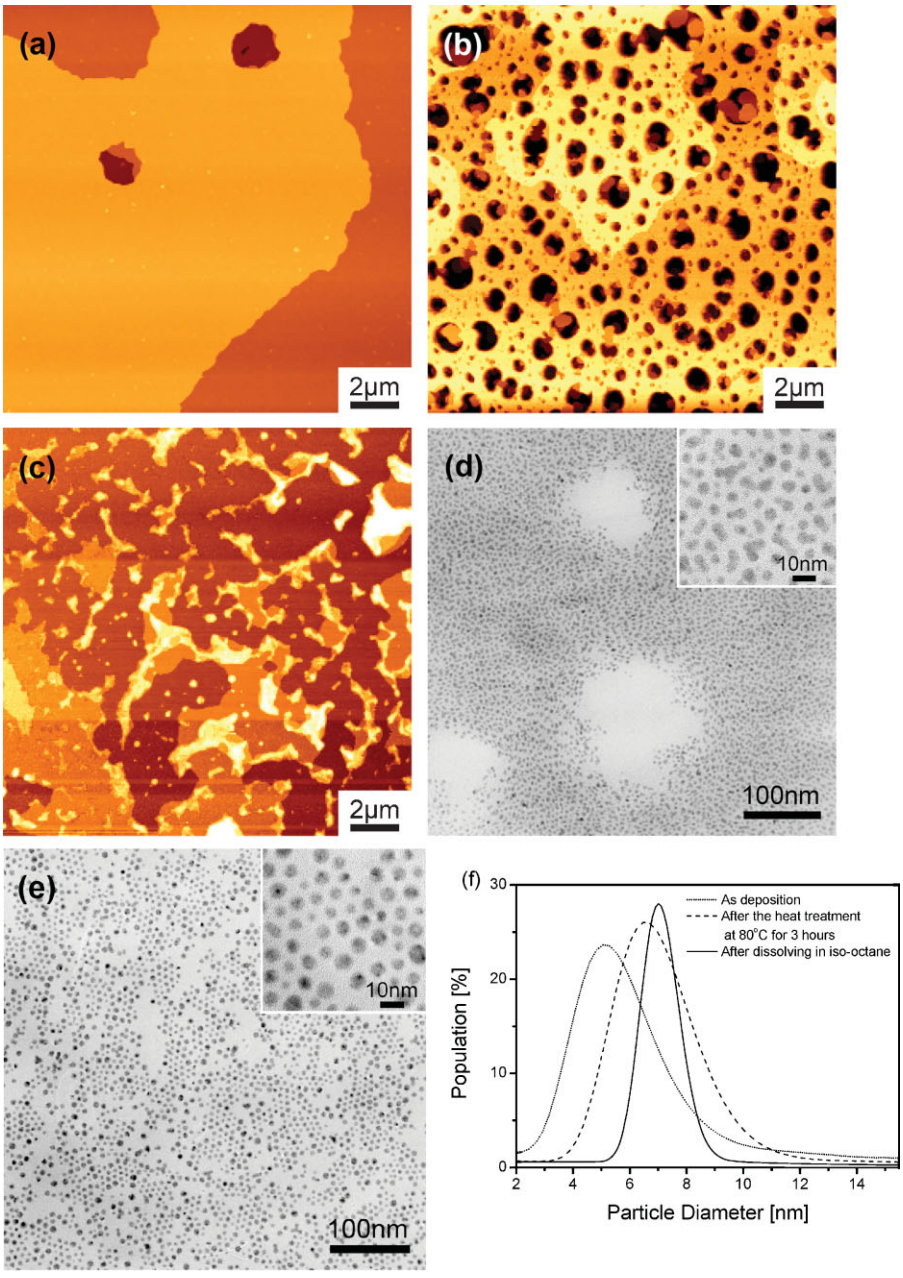

Figure 3. Morphology of the Ag-embedded DOPC membrane. a-c) AFM images of the lipid membrane: a) prior to Ag deposition, b) after Ag deposition, and c) after heat-treatment at 80 °C for 3 h. d,e) TEM plane-view images of the lipid membrane: d) after Ag deposition and e) after heat-treatment at 80 °C for 3 h. Insets represent magnified images of respective Ag nanoparticles samples. f) Size distribution curves of the Ag nanoparticles produced under different conditions.

migration of the lipids and also from the volume expansion resulting from the embedding of the Ag particles. The change in the surface structure of the DOPC membrane was also observed in the X-ray reflectivity measurements (see Supporting Information). When heat-treated at 80 °C, however, the AFM image, Figure 3c, shows that the voids in the DOPC membrane were completely removed as the lipid molecules rearranged themselves to produce a nearly flat surface. The AFM image clearly attests to the high mobility of the lipid molecules during deposition and their ability to rearrange themselves to produce an equilibrium surface structure when provided with increased mobility.[20] In fact, the lateral diffusion coefficient of the DOPC in a bilayer is estimated to be $2 \times 10^{-11}\ m^2\ s^{-1}$,[21] which would give a typical diffusion length scale of 1 μm at 80 °C. Such a high lateral diffusion rate corroborates that the lipid molecules migrated to rearrange themselves. Low-magnification TEM images of the as-deposited and heat-treated samples in Figure 3d and e agreed well with the AFM result. While huge voids interspersed among well-distributed Ag nanoparticles were observed in the as-deposited state, the heat-treatment completely removed those voids. In addition to the macroscopic changes resulting from the increased lipid mobility, the magnified images in the insets of Figure 3d and e demonstrate that both the shape and size of the individual Ag particles were altered by the migration of the lipid molecules chemically bound to Ag. After the heat-treatment, the particles attained spherical shapes and the average size slightly increased from (6.0 ± 2.3) nm to (6.7 ± 1.7) nm but with tighter distribution, as can be seen from the particle size distribution curves in Figure 3f. The formation of spherical Ag particles was driven by Rayleigh shape instability as the elongated particles broke apart and, at the same time, the Ag particles experienced coarsening from Ostwald ripening. Both processes were assisted by accelerated material transport from increased lipid mobility. When deposited directly onto a glass substrate, visible coarsening of the pure Ag islands occurred above 300 °C, substantiating the increased rate of material transport by the Ag-attached lipid molecules. The shape alteration of the Ag particles supports that Ag atoms are strongly bound to ionic head group of the molecules. Further evidence for the chemical interaction between the lipid molecules and Ag was provided when Ag-oxide particles were found from extended heat-treatment of the Ag-embedded DOPC membrane.

In order to provide maximum mobility to the lipid molecules and hence to expedite formation of energetically favorable

configurations, the Ag-embedded DOPC membrane was redissolved from the substrate using a nonpolar solvent, iso-octane. As the solvent evaporated, depending on the concentration, structures ranging from 2D to 3D superlattices were produced from the self-assembly of Ag nanoparticles. The TEM images in Figure 4a were obtained by re-dissolving the $2 \times 2\,cm^2$ membrane in 1 mL of iso-octane. The iso-octane was allowed to evaporate until 20 μL of the lipid solution remained in the vial. Then the lipid solution was transferred onto a carbon-coated Cu grid. Figure 4a illustrates the ordered 2D superlattice formed through self-assembly of the lipid-coated Ag nanoparticles. The ordering of the Ag particles was observed over a large area extending up to well over a micrometer. The electron diffraction pattern in the inset was indexed to a face-centered cubic (fcc) structure with lattice parameter of 0.41 nm, verifying that the particles are metallic Ag. The particle size distribution curve estimated from the TEM image shown in Figure 4a clearly attests to the further tightened particle size distribution of the Ag nanoparticles after redissolving in iso-octane. Accompanying the tightened distribution was a slight increase in the average particle size, which rose to (7.0 ± 0.7) nm. The narrow size distribution and increased particle size suggest that there was rapid motion of lipid molecules that led to redistribution of Ag. Time-dependent change of Ag nanoparticles in size and distribution, while dispersed in a solvent, has been previously observed.[12] The high-magnification TEM image in Figure 4b indicates that a nearly regular hexagonal superlattice was generated through ordering of the uniform-sized Ag particles, although a few voids were observed. The interparticle distance (center-to-center) estimated from the Fourier transform of the TEM micrograph in Figure 4b shown in the inset was 11 nm, making the distance between two neighboring particles (edge-to-edge) 4 nm, which is substantially shorter than the typical DOPC bilayer thickness (4–6 nm).[19,20] The distance between two neighboring particles suggests that it is likely that each Ag particle is encapsulated by a single shell of lipid molecules, much like a reverse micelle with the hydrocarbon chains from the lipids interlacing one another. The TEM result suggests that removal of the excess lipids decreased the interparticle distance. In addition to the decreased interparticle distance, the redistribution of Ag through the lipid motion effected the formation of highly ordered secondary structure. In some

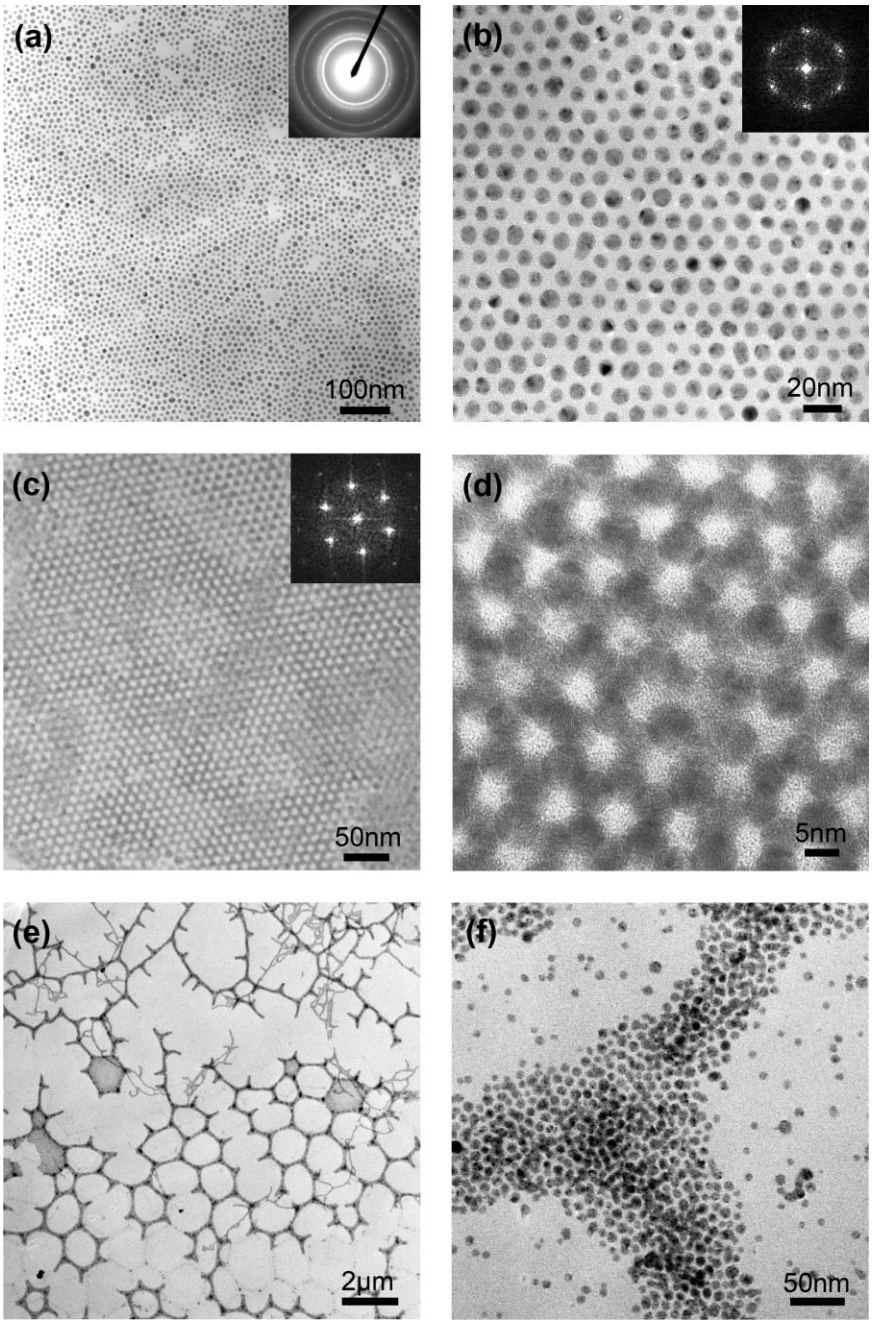

Figure 4. TEM images of various structures formed by the lipid-encapsulated Ag nanoparticles. a) TEM image of 2D self-assembled Ag nanoparticles formed after dissolving in iso-octane (inset: electron diffraction pattern of the sample). b) Magnified image of (a). c) TEM image of 3D self-assembled Ag nanoparticles formed after dissolving in iso-octane. d) Magnified image of (c). e) Low- and f) high-magnification images of the ''honeycomb'' structure formed by dissolving the Ag-embedded membrane in chloroform. The insets in (b) and (c) show the Fourier transform of the respective images.

ADVANCED MATERIALS

regions, as can be seen in Figure 4c, the Ag nanoparticles were nearly monodisperse. The monodispersity enabled highly regular hexagonal arrangement of the Ag nanoparticles (as verified by Fourier transform of the image shown in the inset) upon which another layer of the Ag nanoparticles were stacked to create a 3D superlattice. The second layer of Ag nanoparticles located on top of the interstices of the bottom layer can be clearly discerned from the magnified TEM micrograph in Figure 4d. It is remarkable that the irregular elongated Ag particles in the as-deposited state as seen in Figure 3d crystallized into a highly regular lattice in Figure 4c by imparting increased mobility to the lipids which facilitated redistribution of Ag atoms.

Dissolving the Ag-embedded lipid membrane in a polar solvent, chloroform, also resulted in the formation of ordered superlattices, but with increased density of mis-registered Ag particles. It appears that in a polar solvent, the head group of lipids may have detached themselves from the Ag nanoparticles, preventing formation of a highly-ordered superlattice. However, a complex superstructure was formed when 10 ml of chloroform was dropped on the Ag-embedded membrane and immediately transferred onto a carbon-coated Cu grid using a pipette. In this case, instead of forming a continuous particle layer, a honeycomb-like superstructure was generated as shown in Figure 4f. The bridges forming the honeycomb-like superstructure were composed by a dense mono- or multi-layer of nearly monodisperse Ag nanoparticles as can seen in Figure 4f. The "honeycomb" structure may be related to the transition of the lipid liquid crystal to the reverse hexagonal phase.[22] Development of a similar "honeycomb" structure resulting from the transition of the lipid mesophase to reverse hexagonal phase has been previously reported.[21b] It is conjectured that the freed DOPC molecules arranged into hexagonal shapes while Ag nanoparticles were segregated into the phase boundaries, creating the observed superstructure. Figure 4 presents an interesting possibility that various superstructure can be created as desired using the lipid-encapsulated metal particles by varying the lipid concentration, temperature and solvent.

One of the unique properties of the amphiphilic phospholipids is that the phospholipids are able to form various structures: micelle, vesicle, and planar bilayer.[23] Utilizing this property, we developed a novel approach of using solid-supported lipid membrane to fabricate nano-sized metal particles and simultaneously encapsulate the nanoparticles with lipid molecules. High mobility of the lipid molecules enabled production of uniform-sized Ag nanoparticles. Using these lipid-encapsulated Ag nanoparticles, it was possible to produce various superstructures ranging from a 2D planar superlattice, multi-stacked 3D superlattices and honeycomb-like structure. This method can be easily extended to other noble metals or other transition metals not susceptible to oxidation. The lipid-based template approach to prepare a highly ordered metal particle array demonstrated here can also be useful for creation of a variety of other nano-structures such as nano-biosensor arrays, nano photonic arrays (such as surface plasmon resonance particles), and nano catalyst arrays.

Experimental

For comparison, two different lipids were used. 1,2-dioleoyl-*sn*-glycero-3-phosphatidylcholine (DOPC) with its transition from the intermediate phase to the liquid crystalline phase at −5 °C (in vacuum) [18] should remain a flexible membrane at room temperature. Meanwhile, 1,2-dipalmitoyl-sn-glycero-3-phosphatidylcholine (DPPC) with saturated aliphatic tails phase-transforms to the liquid crystalline state at 98 °C (in vacuum) [18], thus making the solid-supported DPPC membrane relatively rigid at room temperature. Solid-supported DOPC and DPPC membranes were prepared by spin-coating the respective lipid solution onto a Si (or fused silica) substrate following the method devised by Mennicke and Salditt [24]. Lipid solutions were made by dissolving the lipids in chloroform (10 mg mL^{-1}). 100 μL of each lipid solution was used to form the multilayer by spin-coating at 5000 rpm onto a 2×2 cm^2 fused silica substrate. After spin-coating, the solvent was allowed to evaporate in a freeze dryer for 12 hours. A 3 nm thick Ag layer was deposited onto the lipid multilayer using a simple thermal evaporator. The lipid multilayer transferred from the dryer to the chamber which was pumped down to 1×10^{-4} Pa. The film thickness was monitored using a quartz balance to produce the deposition rate of 0.3 Å s^{-1}. Transmission electron microscopy (TEM, JEOL2010), atomic force microscopy (AFM, XE-100), and UV-visible spectrophotometry (UV-vis, UV-2450 from SHIMADZU) were used to characterize the Ag-embedded lipid membrane. For X-ray photoelectron spectroscopy (XPS, PHI 5800), monochromatic X-ray generated from Al Kα (14.7 kV, 33 mA) with beam size of 1×4 μm^2 was used to study structural changes in the Ag-embedded lipid membrane.

Received: February 20, 2008
Revised: April 5, 2008
Published online: August 5, 2008

[1] Y. Zhou, *Curr. Nanosci.* **2006**, *2*, 123.
[2] a) J. G. Brennan, T. Siegrist, P. J. Carroll, S. M. Stuczynski, P. Reynders, L. E. Brus, M. L. Steigerwald, *Chem. Mater.* **1990**, *2*, 403. b) J. I. Abes, R. E. Cohen, C. A. Ross, *Chem. Mater.* **2003**, *15*, 1125.
[3] a) S. Sun, C. B. Murray, D. Weller, L. Folks, A. Moser, *Science* **2000**, *287*, 1989. b) F. X. Redl, K.-S. Cho, C. B. Murray, S. O'Brien, *Nature* **2003**, *423*, 968.
[4] S. Stappert, B. Rellinghaus, M. Acet, E. F. Wassermann, *J. Cryst. Growth* **2003**, *252*, 440.
[5] S. Polarz, A. Roy, M. Merz, S. Halm, D. Schröder, L. Schneider, G. Bacher, F. E. Kruis, M. Driess, *Small* **2005**, *1*, 540.
[6] T. M. Day, P. R. Unwin, J. V. Macpherson, *Nano Lett.* **2007**, *7*, 51.
[7] G. Schmid, in *Nanoparticles: From Theory to Applications* (Ed: G. Schmid), Wiley-VCH, Weinheim, Germany **2004**.
[8] a) C. Mao, D. J. Solis, B. D. Reiss, S. T. Kottmann, R. Y. Sweeney, A. Hayhurst, G. Georgiou, B. Iverson, A. M. Belcher, *Science* **2004**, *303*, 213. b) J. M. Slocik, R. R. Naik, M. O. Stone, D. W. Wright, *J. Mater. Chem.* **2005**, *15*, 749.
[9] a) F. Juillerat, H. H. Solak, P. Bowen, H. Hofmann, *Nanotechnology* **2005**, *16*, 1311. b) H. Y. Lin, L. C. Tsai, C. D. Chen, *Adv. Funct. Mater.* **2007**, *17*, 3182. c) J. Joo, B. Y. Chow, J. M. Jacobson, *Nano Lett.* **2006**, *6*, 2021. d) J. L. Plaza, Y. Chen, S. Jacke, R. E. Palmer, *Langmuir* **2005**, *21*, 1556.
[10] a) D. I. Gittins, F. Caruso, *Angew. Chem. Int. Ed.* **2001**, *40*, 3001. b) T. P. Bigioni, X. M. Lin, T. T. Nguyen, E. I. Corwin, T. A. Witten, H. M. Jaeger, *Nat. Mater.* **2006**, *5*, 265. c) M. L. Kahn, M. Monge, E. Snoeck, A. Maisonnat, B. Chaudret, *Small* **2005**, *1*, 221. d) J. Liu, Y. Li, *Adv. Mater.* **2007**, *19*, 1118.

[11] a) L. E. Euliss, S. G. Grancharov, S. O'Brien, T. J. Deming, G. D. Stucky, C. B. Murray, G. A. Held, *Nano Lett.* **2003**, *3*, 1489. b) B. Dubertret, P. Skourides, D. J. Norris, V. Noireaux, A. H. Brivanlou, A. Libchaber, *Science* **2002**, *298*, 1759. c) N. L. Goicochea, M. De, V. M. Rotello, S. Mukhopadhyay, B. Dragnea, *Nano Lett.* **2007**, *7*, 2281.

[12] S. He, J. Yao, P. Jiang, D. Shi, H. Zhang, S. Xie, S. Pang, H. Gao, *Langmuir* **2001**, *17*, 1571.

[13] a) H. Duan, D. Wang, D. G. Kurth, H. Mohwald, *Angew. Chem. Int. Ed.* **2004**, *43*, 5639. b) F. Reincke, S. G. Hickey, W. K. Kegel, D. Vanmaekelbergh, *Angew. Chem. Int. Ed.* **2004**, *43*, 458. c) Y.-J. Li, W.-J. Huang, S.-G. Sun, *Angew. Chem. Int. Ed.* **2006**, *45*, 2537. d) S. Yun, Y. Park, S. K. Kim, S. Park, *Anal. Chem.* **2007**, *79*, 8584.

[14] D. M. Small, *The Physical Chemistry of Lipids,* Plenum, New York **1986**.

[15] A. Terheiden, C. Mayer, K. Moh, B. Stahlmecke, S. Stappert, M. Acet, B. Rellinghaus, *Appl. Phys. Lett.* **2004**, *84*, 3891.

[16] B. Yang, S. Kamiya, K. Yoshida, T. Shimizu, *Chem. Commun.* **2004**, 500.

[17] T. R. Jensen, M. D. Malinsky, C. L. Haynes, R. P. Van Duyne, *J. Phys. Chem. B* **2000**, *104*, 10549.

[18] A. Terheiden, B. Rellinghaus, S. Stappert, M. Acet, C. Mayer, *J. Chem. Phys.* **2004**, *121*, 510.

[19] V. V. Ginzburg, S. Balijepalli, *Nano Lett.* **2007**, *7*, 3716.

[20] Z. V. Leonenko, E. Finot, H. Ma, T. E. S. Dahms, D. T. Cramb, *Biophys. J.* **2004**, *86*, 3783.

[21] a) A. Filippov, G. Orädd, G. Lindblom, *Langmuir* **2003**, *19*, 6397. b) P. F. Faheyt, W. W. Webb, *Biochemistry* **1978**, *17*, 3046.

[22] J. Barauskas, M. Johnsson, F. Tiberg, *Nano Lett.* **2005**, *5*, 1615.

[23] R. Glaser, *Biophysics*, Springer, New York **2001**.

[24] U. Mennicke, T. Salditt, *Langmuir* **2002**, *18*, 8172.